



OPEN ACCESS

EDITED BY

Qian Sen,
Chinese Academy of Sciences (CAS),
China

REVIEWED BY

Jifeng Han,
Sichuan University, China
Wenjie Wu,
University of California, Irvine,
United States
Yasuhiro Nishimura,
Keio University, Japan

*CORRESPONDENCE

Jingkai Xia,
✉ xiajk@shanghaitech.edu.cn

RECEIVED 07 February 2023

ACCEPTED 06 June 2023

PUBLISHED 15 June 2023

CITATION

Fu Z, Gao F, Wang W and Xia J (2023),
Geomagnetic field effects on the
performance of 8-inch dynode
photomultiplier tubes.
Front. Phys. 11:1160388.
doi: 10.3389/fphy.2023.1160388

COPYRIGHT

© 2023 Fu, Gao, Wang and Xia. This is an open-access article distributed under the terms of the [Creative Commons Attribution License \(CC BY\)](https://creativecommons.org/licenses/by/4.0/). The use, distribution or reproduction in other forums is permitted, provided the original author(s) and the copyright owner(s) are credited and that the original publication in this journal is cited, in accordance with accepted academic practice. No use, distribution or reproduction is permitted which does not comply with these terms.

Geomagnetic field effects on the performance of 8-inch dynode photomultiplier tubes

Zaiwei Fu¹, Feng Gao², Wenwen Wang³ and Jingkai Xia^{4*}

¹China Nuclear Tongchuang (Shanghai) Technology Development Co., Ltd., Shanghai, China, ²Université libre de Bruxelles, Bruxelles, Belgium, ³Huawei Technologies Co., Ltd., Nanjing, China, ⁴Center for Transformative Science, ShanghaiTech University, Shanghai, China

Two different systems have been built to study the geomagnetic field effect on the performance of large area photomultiplier tubes. The main characteristics of photomultiplier tubes such as gain, collection efficiency, transition time spread and energy resolution were measured to investigate the effect. This study shows that both the dynode structure and the orientation of photomultiplier tubes have a large influence on the performance due to the geomagnetic field effect. Different methods were proposed and tested to reduce these effects. The results were obtained with and without high-permeability permalloy foil shielding. It is found that the effect of the geomagnetic field can be significantly reduced by the permalloy foil. The influence of the geomagnetic field under different installation geometries is also studied and discussed in this paper.

KEYWORDS

large area PMT, geomagnetic field effect, shielding, dynode structure, R5912

1 Introduction

Large area dynode-style photomultiplier tubes (PMTs) are very sensitive to magnetic fields. In fact, even geomagnetic field has significant effects on the performance of these large area PMTs [1]. This is mainly due to the long travel distance of photoelectrons inside the PMT. Large area dynode-type PMTs usually have a spherical design with a large distance between the photocathode and the dynode collector [2]. When the photoelectron generated from the photocathode travels to the dynode in a magnetic field, its track is deviated from the orbit due to the Lorentz effect, while the track is also changed between series dynodes. This then affects the performance of the PMT such as the gain, collection efficiency, energy resolution and transition time spread (TTS).

Many articles have studied the geomagnetic field effect on the properties of PMTs with particular relevance to their specific experiment requirements. E. Leonora et al. tested the geomagnetic field effect on properties of Hamamatsu 8" and 10" PMTs in detail for a cubic-kilometer-scale neutrino telescope [3]. E. Calvo et al. studied the effect of the geomagnetic field on PMT using magnetic shielding materials for different parts of the PMT according to the requirements of the Double Chooz experiment [4]. P. DeVore et al. tested the effect of the geomagnetic field on different types of PMTs and used a new shielding material to shield these PMTs, as required for the Daya Bay experiment [5].

The Jiangmen Underground Neutrino Observatory (JUNO) is currently under construction in Jiangmen, China [6], and is to measure the neutrino mass ordering with a precise energy resolution of $3\%/\sqrt{\text{MeV}}$ [6]. To achieve it, JUNO requires that the PMT photocathode coverage is larger than 75%, and the PMT quantum efficiency is better than 35%. Two kinds of 20-inch PMTs will be applied in JUNO experiment: conventional dynode

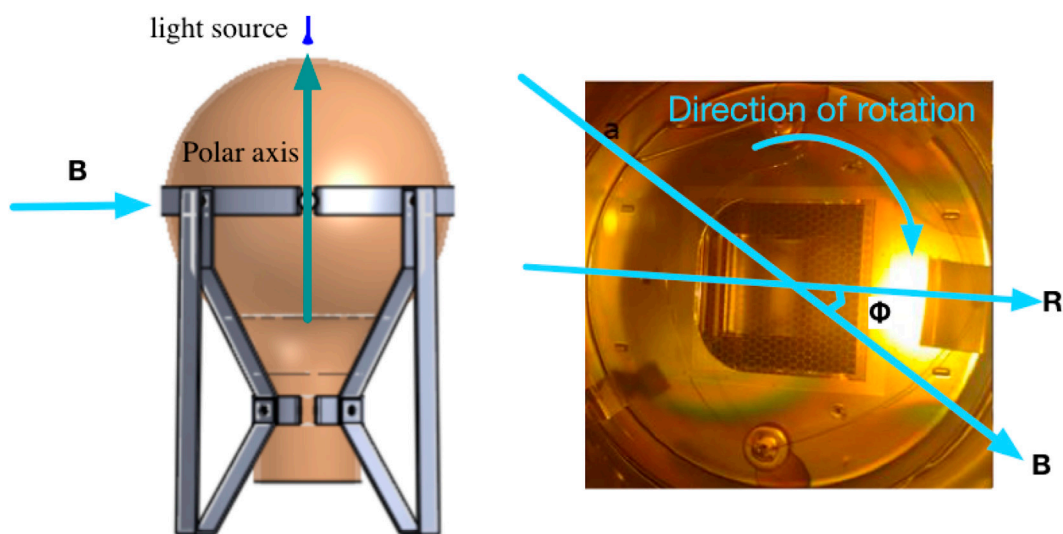


FIGURE 1

Rotation test system. On the left side, the PMT can be rotated around its polar axes while the geomagnetic field and the PMT remain relatively the same. On the right, it is the reference direction of the first dynode.

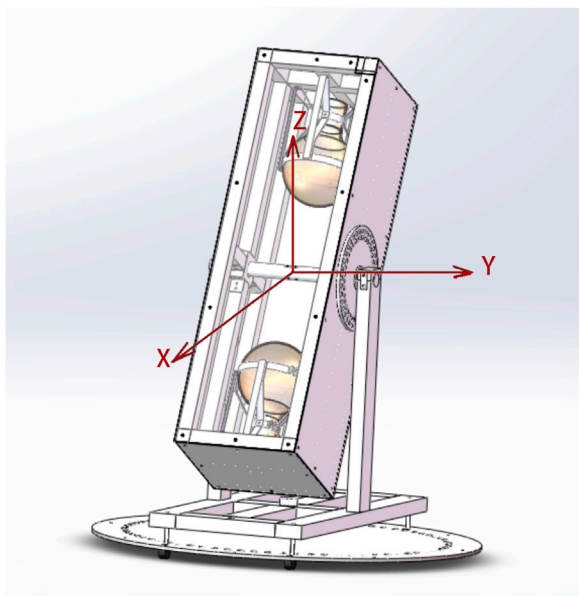


FIGURE 2

Revolution system. This device can bring the PMT rotating around 2π in two plates.

design PMT manufactured by Hamamatsu [7] and new microchannel plate (MCP)-PMT manufactured by North Night Vision Technology (NNVT) [8]. These PMTs will be installed around a spherical acrylic vessel to detect the light emitted from the target inside the vessel. This paper mainly studied the effect of the geomagnetic field on conventional PMTs from Hamamatsu. The measurement system and setup are described in Section 2. The results of the experiments, considering the effects of PMT dynode

design and installation position, are presented and discussed in Section 3, 4 respectively. The conclusions are given in Section 5. Since both the 8-inch R5912 tested in this paper and the 20-inch R12860 used in JUNO is Hamamatsu Box & Line-dynodes tube and have a similar upper bulb shape, the experiment results give guidance of studying the geomagnetic effect on 20-inch PMT.

2 Experiment setup

The PMT used in this experiment is Hamamatsu 8-inch PMT R5912 [9], which operates at a gain of 10^7 . R5912 is a typical type of PMT widely used in high energy physics experiments [5,10,11]. The behavior of the large area PMT in the geomagnetic field is mainly due to the PMT's design and orientation in the magnetic field. As shown in Figure 1, the dynode structure of the PMT is asymmetric. To study the effects of the geomagnetic field from the internal structure of the PMTs, a rotation device was built (see in Section 2.2). To investigate the effects when PMT is installed toward to different directions, a revolution device was built (see Section 2.3).

2.1 The measurement system

The critical parameters to describe the geomagnetic field effects on the PMTs includes the gain, collection efficiency (CE), energy resolution (ER) of the single photoelectron (SPE) spectrum, and the transition time spread (TTS), which is also tested under SPE mode of the PMTs. In this experiment, the incident light is provided by a 405 nm laser diode which has the advantages of a small divergence angle and minimum time delay. The SPE spectrum can be obtained by modifying its light intensity by adjusting the voltage, duty ratio and frequency of the power supply. The spectrum is measured with a Charge-to-Digital Converter (QDC). An event counter is used to

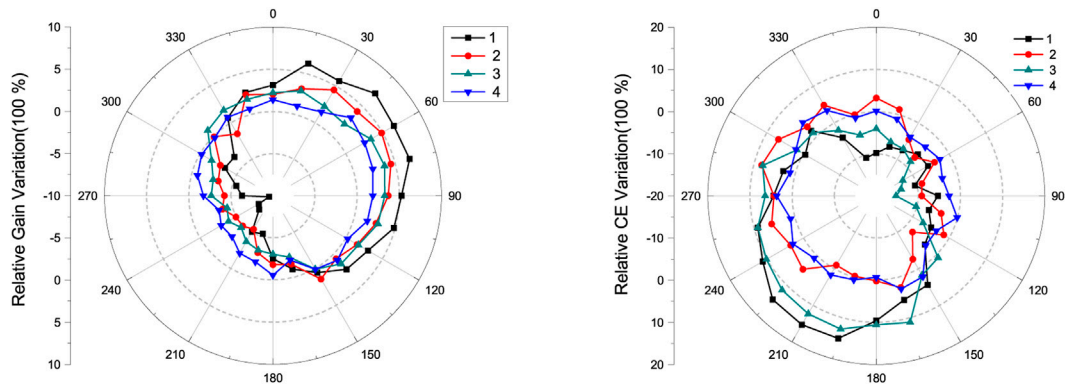


FIGURE 3

Geomagnetic effect on different parts of the PMT. 1) no shielding, 2) upper shielding: covering only the region above the PMT equator, 3) lower shielding: covering only the region below the PMT equator, 4) full shielding: covering the entire PMT bulb.

TABLE 1 The maximum, the average and the minimum relative variation [unit: %] of PMT properties with/without shielding when the PMT rotating around its polar axis.

Variation	Minimum		Maximum	
	Non	Shield	Non	Shield
Gain	-21.32	-4.48	13.49	9.91
CE	-15.27	-4.60	19.58	6.70
ER	-17.77	-10.61	44.68	9.55
TTS	-13.33	-3.30	26.20	4.80

calculate the relativity collection efficiency. A time-to-digital converter (TDC) module is used to measure the TTS with a resolution of 35 ps/LSB.

2.2 The rotation device

In the rotation device, the PMT is mounted on a horizontally placed holder, with the polar axis parallel to the vertical plane. Figure 1 (left) is a front view of the set-up. It brings the PMT rotating along its polar axis. When rotating the PMT, the incident light and PMT location keep the same but the dynode direction changes with respect to the local geomagnetic field. The PMT reference direction is shown on the right in Figure 1, denoted as R, is drawn from the center of the arc edge of the focus to the center of the PMT. The angle between the PMT reference direction and the horizontal component of the geomagnetic field B is denoted by ϕ when the PMT rotates clockwise.

In this test system, the emission direction of the photoelectrons does not change relative to the geomagnetic field. However, the relative position of the PMT structure changes when the PMT rotates around its polar axes. Therefore, the output signal varies with the change of the angle ϕ between the reference direction and the local geomagnetic field.

2.3 The revolution device

In a large area PMT, the distance between the photocathode and the first dynode is quite large, and the photoelectron path is strongly affected by the geomagnetic field when it travels from the photocathode to the first dynode. Due to the above effect, the energy and direction of the incident electrons are not uniform anymore. Hence the secondary electron emission coefficient, the gain, as well as the CE, of the PMT vary a lot in different situations. For example, when large area PMTs with the same structure are installed at different positions, the angle of illuminating light and the geomagnetic field will be different, and the photoelectron flying track affected by the geomagnetic will also be different. So a revolution device (shown as Figure 2) is designed to study how the installation position of the PMT contributes to its characteristics in the geomagnetic field.

The rotation components were composed of two parts: the dark box which could rotate around 2π in the vertical direction, and a horizontal rotation plate which could rotate around 2π in the horizontal direction below the base. Two 8-inch PMTs can be installed in this device for simultaneous test with point-like light illumination. So in this device, a dark box could bring the PMTs and rotate around 4π manually.

2.4 The shielding of the geomagnetic field

There are two ways to reduce the influence of geomagnetic field on PMT: high permeability permalloy shielding and coil compensation [4,5,12]. In the experiment, permalloy shielding was used to reduce the geomagnetic field effect on PMT with the advantage that the geomagnetic field could be selectively blocked based on the specific influence of different azimuths of the PMT.

The shielding materials were rolled into a cylinder and can cover the entire PMT. The direction of the cylinder is always parallel to the polar axes of the PMT. When the local geomagnetic field is about $38.04 \mu\text{T}$, the residual intensity of the geomagnetic field after shielding is reduced to $12.12 \mu\text{T}$.

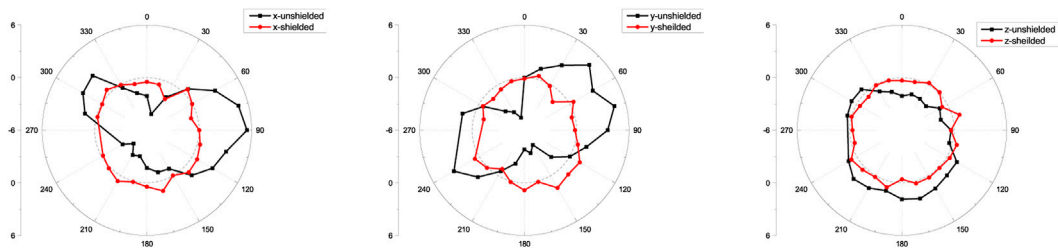


FIGURE 4
Gain variation with the PMT rotating around x , y and z -axes.

3 The construct factor of the PMT in the geomagnetic field

3.1 The PMT construct contribution

The process of the geomagnetic field effect on photoelectrons in a PMT can be divided into two steps. First, the photoelectron is deviated from the focus by Lorentz force when it travels from the photocathode to the focus, resulting in a decrease in the collection efficiency of the PMT. Secondly, part of the secondary electrons will drift from the effective multiplication area under the action of Lorentz force from the focus to the anode, which will result in the loss of PMT gain [3]. Meanwhile, TTS and ER are also influenced by the geomagnetic field. TTS is affected due to the variation in electron trajectory during travel, which in turn affects the flight time of electrons. ER is affected because the gain of the PMT directly impacts the ER [13].

Considering different properties are related to different parts of the PMT, studies have also been done on the relationship between shielding different parts of the PMT and the performance of the PMT. The relative variation of the performance is given as $\frac{val-average}{average}$, where val represents the values of gain or CE at different angles, and $average$ is the average value of these values across all angles. Figure 3 shows the performances of the PMT in the cases of 1) no shielding, 2) upper shielding: covering only the region above the PMT equator, 3) lower shielding: covering only the region below the PMT equator, 4) full shielding: covering the entire PMT bulb. It can be seen that gain has a strong relationship with the bottom of the PMT, while CE is mainly affected by the distance between the photocathode and the focus with the largest relative variation up to $\pm 15\%$.

3.2 The dynode structure contribution

The PMT itself, especially dynodes, is not a strict symmetrical geometric structure, resulting in an asymmetric electric field. The directions and values of the total electric and Lorentz forces from the same point are different when PMT rotates around its polar axis.

In the rotation test system, photoelectrons are emitted in the same direction when the PMT rotates around its polar axes since the light is fixed relative to the rotation axes. The PMT properties such as gain, CE, ER and TTS vary while the PMT rotates due to the PMT's structure asymmetry. Table 1 lists the results of obtained PMT properties with and without shielding. It can be known that PMT's structure asymmetry

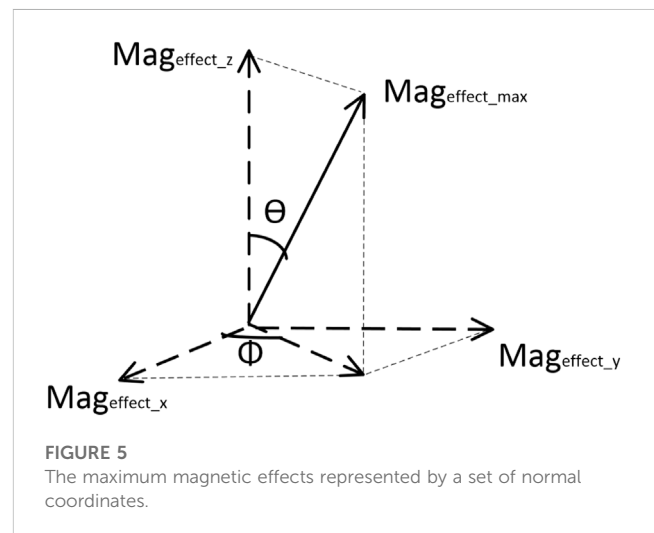


FIGURE 5
The maximum magnetic effects represented by a set of normal coordinates.

has a great contribution to the influence of the geomagnetic field on the PMT performance. The maximum and the minimum relative variation of PMT gain are around $+14\%$ at $\phi = 315^\circ$ and -22% at $\phi = 240^\circ$ respectively. The maximum and the minimum relative variation of CE are around $+20\%$ at $\phi = 90^\circ$ and -15% at $\phi = 315^\circ$. Clearly, the asymmetric design of a PMT cannot be ignored when considering its performance in the magnetic effect.

4 The installation position of the PMT in the geomagnetic field

4.1 The affection to the PMT characteristics

In the revolution device, the PMT can be rotated in any plane. Three vectors: \vec{x} , \vec{y} and \vec{z} are used to represent the directions of these planes, where \vec{x} is the direction of the longitudinal plane, \vec{y} is the direction of the latitudinal plane, and \vec{z} is the direction of the horizontal plane, as shown in Figure 2. The direction of the electric field varies when the PMT rotates around an axis, which leads to the change in the direction and the value of the total electric and Lorentz forces. Properties such as gain, CE, ER and TTS also vary following the variation of the total force. Figure 4 shows the gain variation with PMT rotating around x , y and z -axes, respectively. During the experiment, the PMT rotates 360° within three

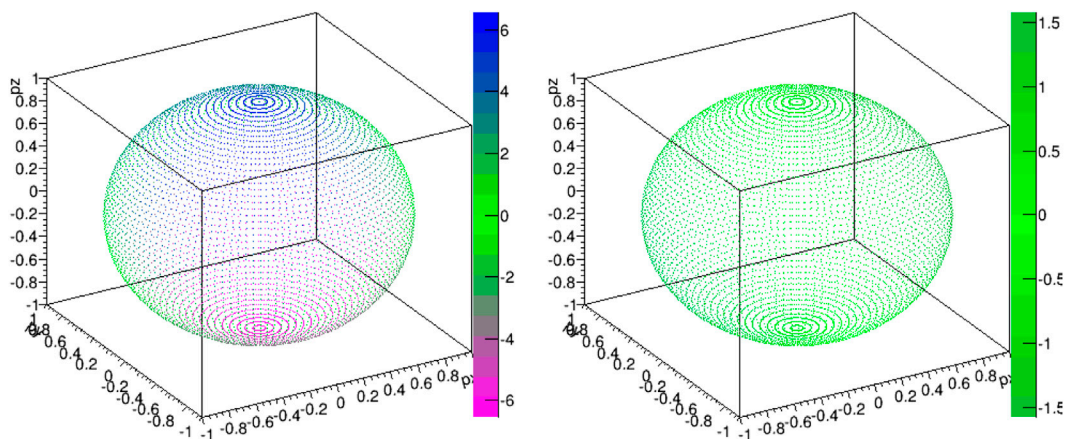


FIGURE 6
Geomagnetic field effects on the property of gain of the PMT. The colour bar represent the relative variation [unit: %].

orthogonal planes, so each 0° represents a chosen starting point within that plane. When one of the three angles changes, the other two remain constant. The largest relative gain variation is about $\pm 5\%$ without shielding and within $\pm 2\%$ with permalloy shielding. By comparing the results in Table 1 and Figure 4, we found that PMT asymmetry has a larger contribution to the geomagnetic effect on the PMT performance than the installation position of the PMT.

4.2 Geomagnetic effect on a sphere surface

The geomagnetic field strength \vec{v} can be uniquely represented by a set of vectors in the three-dimensional orthogonal plane. The effect on the PMT has the maximum value with the electron path being perpendicular to the direction of the geomagnetic field. This maximum effect can also be represented by a set of normal orthogonal coordinate vectors. Figure 5 shows the direction of the maximum magnetic effect $Mag_{effect\ max}$ and its representation by a set of normal orthogonal coordinate vectors.

The effects of the geomagnetic field distributed around the surface of a sphere can be obtained by resolving the maximum effect into different components in different directions around the surface of the sphere. Eq. 1 is an arbitrary vector of the geomagnetic field effect on the PMT in a fixed direction on the surface of the sphere.

$$Mag_{effect} \begin{bmatrix} \sin \theta \cos \varphi \\ \sin \theta \sin \varphi \\ \cos \theta \end{bmatrix} = \begin{bmatrix} Mag_{effect-X} \\ Mag_{effect-Y} \\ Mag_{effect-Z} \end{bmatrix} \quad (1)$$

From the data of the revolution system, the geomagnetic effect on the PMT around the surface of a sphere can be induced by Eq. 1. By using this method, the distribution of the effect of the unshielded/shielded geomagnetic field on the gain of the PMT across the entire plane is shown in Figure 6. Within the plane perpendicular to the magnetic field, there are maximum positive and maximum negative effects from the geomagnetic field. The largest relative gain variation is about $\pm 6\%$ without shielding shown on the left of Figure 6. After

employing permalloy shielding materials, the largest relative gain variation is about $\pm 2\%$ shown on the right of Figure 6.

5 Summary

The geomagnetic effects on the performance of PMTs have been studied with two different test systems: rotation test system and revolution test system. It is found that the asymmetry of the PMT structure is a significant factor in the geomagnetic effect on a PMT, and the PMT can be placed in a specific orientation to reduce the effect caused by asymmetrical structure in the geomagnetic field. The effect of the geomagnetic field on the PMTs varies with its installation direction. By using permalloy shielding, the uniformity of the PMT's performance can be improved when PMT or its dynode is oriented in different directions.

Data availability statement

The original contributions presented in the study are included in the article/supplementary material, further inquiries can be directed to the corresponding author.

Author contributions

ZF designed the experiment, analyzed the data, and provided the funding. WW and JX performed the experiments. FG and JX analyzed the data and prepared the manuscript. All authors contributed to the article and approved the submitted version.

Funding

The project is supported by Science and Technology Program of Shanghai (Grant No. 22ZC2420700).

Acknowledgments

The authors would like to thank Junqi Xie, assistant physicist at Argonne National Laboratory for his help and suggestions on this work. This work is supported by the PMT Laboratory in IHEP.

Conflict of interest

Author ZF was employed by the China Nuclear Tongchuang (Shanghai) Technology Development Co., Ltd; Author WW was employed by the Huawei Technologies Co., Ltd.

References

- Koblesky T, Roloff J, Polly C, Peng J. Cathode position response of large-area photomultipliers under a magnetic field. *Nucl Instr Methods Phys Res Section A: Acc Spectrometers, Detectors Associated Equipment* (2012) 670:40–4. doi:10.1016/j.nima.2011.12.054
- Hamamatsu. *Large photocathode area photomultiplier tubes* (2023). Available at: https://www.hamamatsu.com/content/dam/hamamatsu-photonics/sites/documents/99_SALES_LIBRARY/etd/LARGE_AREA_PMT_TPMH1376E.pdf (Online; accessed May 16, 2023).
- Leonora E, Consortium K. Terrestrial magnetic field effects on large photomultipliers. *Nucl Instr Methods Phys Res Section A: Acc Spectrometers, Detectors Associated Equipment* (2013) 725:148–50. doi:10.1016/j.nima.2012.12.056
- Calvo E, Cerrada M, Fernandez-Bedoya C, Gil-Botella I, Palomares C, Rodríguez I, et al. Characterization of large-area photomultipliers under low magnetic fields: Design and performance of the magnetic shielding for the double chooz neutrino experiment. *Nucl Instr Methods Phys Res Section A: Acc Spectrometers, Detectors Associated Equipment* (2010) 621:222–30. doi:10.1016/j.nima.2010.06.009
- DeVore P, Escontrias D, Koblesky T, Lin C, Liu D, Luk KB, et al. Light-weight flexible magnetic shields for large-aperture photomultiplier tubes. *Nucl Instr Methods Phys Res Section A: Acc Spectrometers, Detectors Associated Equipment* (2014) 737:222–8. doi:10.1016/j.nima.2013.11.024
- Abusleme A, Adam T. JUNO physics and Detector. *Prog Part Nucl Phys* (2021) 123:103927. doi:10.1016/j.pnpnp.2021.103927
- Hamamatsu. *R12860* (2023). Available at: https://www.hamamatsu.com/eu/en/product/optical-sensors/pmt/pmt_tube-alone/head-on-type/R12860.html (Online; accessed May 16, 2023).
- Wang Y, Qian S, Zhao T, Tian J, Li H, Cao J, et al. A new design of large area mcp-pmt for the next generation neutrino experiment. *Nucl Instr Methods Phys Res Section A: Acc Spectrometers, Detectors Associated Equipment* (2012) 695:113–7. doi:10.1016/j.nima.2011.12.085
- Hamamatsu. *R5912* (2023). Available at: <http://pdf.datasheetcatalog.com/datasheet/hamamatsu/R5912.pdf> (Online; accessed May 16, 2023).
- Abeysekara A, Alfaro R, Alvarez C, Álvarez J, Arceo R, Arteaga-Velázquez J, et al. *The hawc gamma-ray observatory: Design, calibration, and operation*, 33rd International Cosmic Ray Conference, Rio de Janeiro, Brazil (2013). *arXiv preprint arXiv:1310.0074*.
- Caldwell T, Seibert S, Jaditz S. Characterization of the r5912-02 mod photomultiplier tube at cryogenic temperatures. *J Instrumentation* (2013) 8:C09004. doi:10.1088/1748-0221/8/09/c09004
- Ghazikhani V, McDonald KT. *μ-metal wire magnetic shields for large pmts* (2007). Available at: https://www.researchgate.net/publication/268259966_m-Metal_Wire_Magnetic_Shields_for_Large_PMTs.
- Gao F, Qian S, Ning Z, Wang Z, Ma L, Yao Z, et al. Data acquisition system for single photoelectron spectra of photoelectric detector. *Nucl Tech* (2019) 42:55–62. doi:10.11889/j.0253-3219.2019.hjs.42.100404

The remaining authors declare that the research was conducted in the absence of any commercial or financial relationships that could be construed as a potential conflict of interest.

Publisher's note

All claims expressed in this article are solely those of the authors and do not necessarily represent those of their affiliated organizations, or those of the publisher, the editors and the reviewers. Any product that may be evaluated in this article, or claim that may be made by its manufacturer, is not guaranteed or endorsed by the publisher.